



OPEN

SUBJECT AREAS:

PHYSICAL SCIENCES

APPLIED PHYSICS

CONDENSED-MATTER PHYSICS

MECHANICAL AND STRUCTURAL
PROPERTIES AND DEVICES

Correlation between micrometer-scale ripple alignment and atomic-scale crystallographic orientation of monolayer graphene

Jin Sik Choi^{1,4*}, Young Jun Chang^{2*}, Sungjong Woo^{3*}, Young-Woo Son³, Yeonggu Park¹, Mi Jung Lee¹, Ik-Su Byun¹, Jin-Soo Kim^{1,4}, Choon-Gi Choi⁴, Aaron Bostwick⁵, Eli Rotenberg⁵ & Bae Ho Park¹

Received

21 October 2014

Accepted

11 November 2014

Published

1 December 2014

Correspondence and requests for materials should be addressed to Y.-W.S. (hand@kias.re.kr) or B.H.P. (baehpark@konkuk.ac.kr)

* These authors contributed equally to this work.

¹Division of Quantum Phases and Devices, Department of Physics, Konkuk University, Seoul 143-701, Korea, ²Department of Physics, University of Seoul, Seoul 130-743, Korea, ³Korea Institute for Advanced Study, Seoul 130-722, Korea, ⁴Creative Research Center for Graphene Electronics, Electronics and Telecommunications Research Institute (ETRI), Daejeon 305-700, Korea, ⁵Advanced Light Source (ALS), E. O. Lawrence Berkeley National Laboratory, Berkeley, California 94720, USA.

Deformation normal to the surface is intrinsic in two-dimensional materials due to phononic thermal fluctuations at finite temperatures. Graphene's negative thermal expansion coefficient is generally explained by such an intrinsic property. Recently, friction measurements on graphene exfoliated on a silicon oxide surface revealed an anomalous anisotropy whose origin was believed to be the formation of ripple domains. Here, we uncover the atomistic origin of the observed friction domains using a cantilever torsion microscopy in conjunction with angle-resolved photoemission spectroscopy. We experimentally demonstrate that ripples on graphene are formed along the zigzag direction of the hexagonal lattice. The formation of zigzag directional ripple is consistent with our theoretical model that takes account of the atomic-scale bending stiffness of carbon-carbon bonds and the interaction of graphene with the substrate. The correlation between micrometer-scale ripple alignment and atomic-scale arrangement of exfoliated monolayer graphene is first discovered and suggests a practical tool for measuring lattice orientation of graphene.

At finite temperature, two-dimensional crystals such as graphene are believed to display structural fluctuations in order to account for their stability¹. Given that graphene is a soft and atomically thin material exhibiting membrane-like features, it is subject to out-of-plane distortions due to thermal fluctuations together with external forces such as interactions with a substrate². Many theoretical^{3–6} and experimental^{7–11} studies have demonstrated that out-of-plane deformations especially ripples are formed on both supported and suspended graphene samples. Ripples affect the electronic properties of graphene in many ways such as modification in the electronic structure¹², induction of large pseudo-magnetic field^{13,14}, local shift of the electrochemical potential¹⁵, etc. Furthermore, periodic ripples give rise to electronic superlattices^{12,15} leading to highly anisotropic charge-carrier velocities¹⁶. Ripples can also alter the mechanical characteristics of graphene. In our previous work, it has been reported that a supported single layer graphene reveals anisotropic friction caused by ripples on it^{17,18}. Because the ripples formed on graphene have small aspect ratio (<1/10) between height (~Å) and width (~nm), their direct detection is beyond atomic force microscopy (AFM) resolution^{17,19}. We believe that similar behaviors related to ripples are expected in many atomically two-dimensional materials. For development and design of devices based on unique electrical and mechanical properties of atomically two-dimensional materials, it is required to find atomistic origin of ripples.

On the other hand, the electronic structure of finite-size graphene strongly depends on the crystallographic orientation of its edges^{16,20–22}. The presence of electronic edge states and localized spins in the zigzag edge region give rise to electronic, magnetic, and chemical activities²³. The identification of crystallographic axis is, therefore, necessary for the characterization and fabrication of finite-size graphene as well as for the development of graphene-based devices.

In this paper, we experimentally and theoretically demonstrate that ripples in a single-layer graphene, mechanically exfoliated on a SiO₂ substrate, are formed preferentially along the zigzag directions of the hexagonal



lattice of graphene. The direction of ripples is determined using cantilever torsion microscopy (CTM)⁵, while the crystallographic axis of graphene is measured using angle-resolved photoemission spectroscopy (ARPES). CTM is a generalized version of friction-mode to observe the ripple domains on exfoliated monolayer graphene by combining two measurements observing cantilever torsions during lateral (T_{LAT}) and longitudinal (T_{LON}) scans in AFM¹⁸. T_{LAT} is known as lateral force microscopy (LFM) or friction force microscopy (FFM) which has been used to investigate the friction force between AFM tip and surface. T_{LON} is known as transverse shear microscopy (TSM)^{24–26} which has been specifically used in determining grain orientation of polycrystalline organic semiconductors. With the CTM and ARPES data obtained from the same sample, we associate the ripple directions to the crystallographic orientation of graphene. Our findings are consistent with our theoretical model which shows that a zigzag-directional ripple is preferred energetically at room temperature over an armchair-directional one. It is worthwhile to note that our fast and simple CTM technique using AFM for macroscopic graphene samples decides the crystallographic orientation of graphene efficiently.

Results

CTM measurements for ripple direction determination. The single-layer graphene ('SLG' in Fig. 1a) used in our analysis is bar-shaped with a longitudinal length of $\sim 85 \mu\text{m}$ (Supplementary Fig. 1)

which is extruded from a multi-layer graphene ('MLG' in Fig. 1a). We took CTM images for two areas on the SLG region of the sample (the red rectangles (i) and (ii) in Fig. 1a). For both of the rectangular areas, the longitudinal (T_{LON}) and lateral (T_{LAT}) CTM images, which are the intensities of local torsion values of the AFM cantilever scanning across the surface of the material, show three-colored domain structures (Fig. 1b). The CTM images reveal local ripple directions. It is observed that the contrasts of the T_{LON} and T_{LAT} images for the area (i) are the same as those for the area (ii). It implies that each scanned area consists of three domains with characteristic ripple directions, while each domain in the area (i) denoted by a color-filled rectangle in Fig. 1b has a corresponding domain in the area (ii) with the same ripple direction. Following the procedure in Ref. 18 with the obtained CTM images, one can determine the range of ripple directions (Supplementary Fig. 2). The rightmost column of Fig. 1b shows the estimated ripple directions with angular resolution of 30° as blue, red and black-colored fans in the pie charts. Each color refers to a domain denoted by the same-colored rectangle in the CTM images. We follow the definition of the ripple direction as indicated in the upper inset of Fig. 1b.

The 60° rotation of ripple directions between adjacent domains supports the notion that the ripples are aligned along a stiff direction of hexagonal graphene lattice, probably zigzag or armchair directions¹⁸. If the lattice orientation of graphene is determined and compared with the ripple directions obtained from CTM, one can

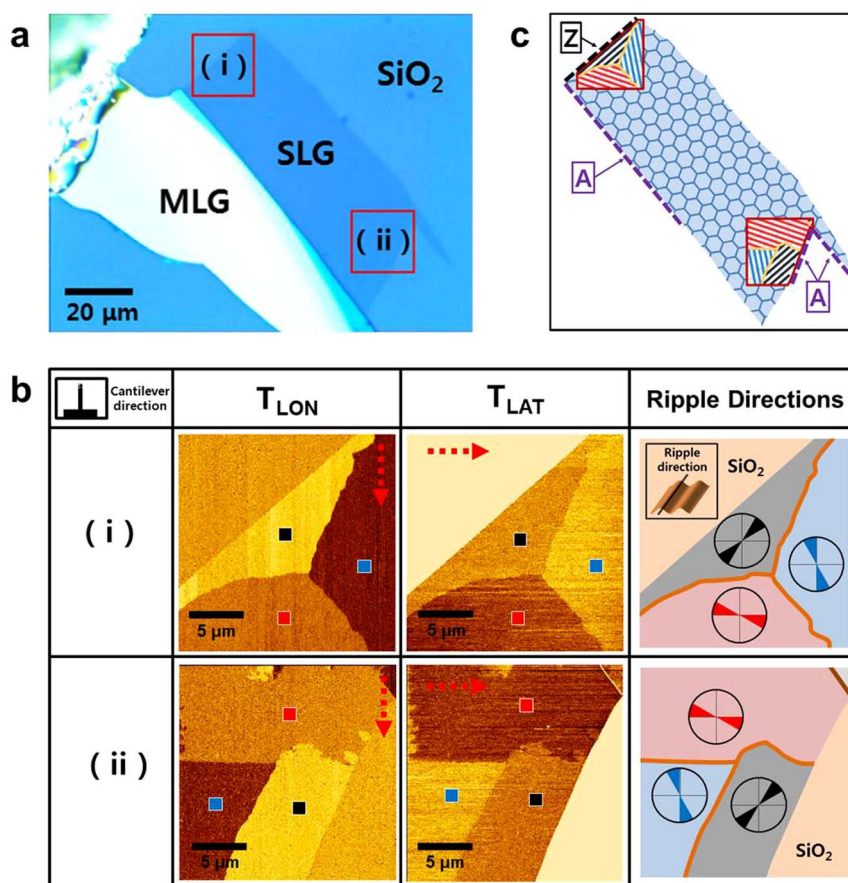


Figure 1 | Relation between graphene crystallographic axis and its ripple directions. (a) Optical microscopy image of multi-layer graphene (MLG) and single-layer graphene (SLG) mechanically exfoliated on SiO_2 . (b) Longitudinal (T_{LON}) and lateral (T_{LAT}) CTM images obtained at areas (i) and (ii) denoted in (a) and the estimated ripple directions. The cantilever direction from the top view is shown in the left upper inset of (b) and the scan direction is indicated by red-dashed arrows. The fan-shaped colored area of each pie chart in the rightmost column of (b) indicates the range of ripple direction for each domain. In the upper inset of the rightmost column of (b), the definition of ripple direction is given as a solid line. (c) The ripple directions in region (i) and (ii) estimated by the CTM images are drawn in as blue, red, and black lines over the schematic figure of hexagonal lattice determined by ARPES. It is noted that zigzag (Z, black dashed line) and armchair (A, purple dashed line) edges are easily identified.



estimate the correlation of crystallographic axis to the directions of ripples in graphene, as shown in Fig. 1c. For this, we use ARPES to determine the lattice orientation of the same graphene sample used for CTM. The usual stick-slip mode of AFM was used for observing the atomic arrangement of graphene which is flat and firmly stuck to the bulk substrate, for example, graphene grown on copper foil²⁷ or SiC²⁸. In case of the exfoliated graphene on SiO₂, the stick-slip images are distorted due to the structural deformation of graphene near an AFM tip during its scanning and cannot lead to clear determination of the crystal structures^{17,29}. The sample used for the CTM is grounded electrically and placed in an ultra-high vacuum chamber. Using optical microscopy and scanning photoemission mapping with step size of $\sim 50 \mu\text{m}$, we locate the small area of interest in the sample. We then use the optical microscopy images of the silver paint region (Supplementary Fig. 1) to align the orientation of the ARPES maps with the CTM data.

ARPES measurements for identifying crystallographic orientation.

The valence and conduction bands in the electronic structure of a SLG meet only at the corners of hexagonal Brillouin zone giving two distinguishable Dirac points, K and K'³⁰. The crystallographic orientation of graphene can be determined by locating the K and K' points in the ARPES maps (Figs. 2a and 2b). The energy band obtained from the ARPES shows a nearly linear energy dispersion along the Γ -K direction agreeing well with the previous measurements^{30–35} (Supplementary Fig. 3). Figures 2c and 2d show the optical microscopy image and the ARPES map of our graphene sample, respectively. For the sample aligned using the silver paint, the constant energy scan at the Fermi level shows four peaks corresponding to the K and K' points of graphene (Fig. 2d)^{31–35}. From this ARPES map, the hexagonal Brillouin zone boundary connecting six K and K' points is determined. The black solid arrows in Figs. 2a–2d show the zigzag direction of graphene

atomic structure decided from the positions of the measured K and K' points in Fig. 2d, while the black dashed arrow in Fig. 2d denotes the Γ -K direction.

Now, by superimposing the ripple directions determined from the CTM on the crystallographic axis obtained from the ARPES, we find that zigzag directions are within the range of estimated ripple directions for all the three ripple domains; ripples are aligned along the zigzag directions of the graphene lattice (Fig. 1c). In Fig. 1c, one can readily distinguish zigzag and armchair edges. This is important from the practical point of view since it implies that CTM technique based on conventional AFM can be used as a facile method to determine the crystallographic orientation and edge structures of graphene at normal temperature and pressure.

Theoretical calculations of ripple formation energy. We have also performed theoretical calculations to find the difference in energies required to form zigzag- and armchair-directional ripples as well as to estimate the equilibrium width of ripple on a substrate. When graphene is adhered to a substrate, ripples can be formed due to external strain forces¹⁰. Especially mechanical exfoliation accompanies heating and cooling, which introduce compressive strain in graphene^{36,37}. Once ripple domains are formed due to external strain forces, they tend to remain³⁸. The rippling deformation of supported graphene due to the compressive strain from the substrate should be nearly conformal since the σ bond that determines the C–C bond length is much stiffer than the out-of-plane-oriented π bond. The rippling energy is obtained by integrating the local energy cost due to the curvature of the ripple³⁹. A given compressive strain fixes the ratio of ripple height to the ripple width. A larger ripple width gives an overall smaller curvature leading to lower rippling energy which, in contrast, causes an increase in the ripple height thereby causing its interaction energy with the substrate to increase. The competition between these two energies determines the width of the graphene ripple on a substrate. The graphene-substrate interaction energy is estimated by integrating the local interaction between graphene and the substrate using Lennard-Jones potential with parameters obtained experimentally⁴⁰. Under a compressive strain of $\sim 10\%$, we find that the ripple width is approximately 5.7 nm and that the zigzag-directional ripple has a lower energy than the armchair-directional one by 0.16 meV nm^{-2} (Fig. 3). Considering that the observed size of the ripple domain is several tens of μm^2 , the energy difference for a ripple domain (\sim several keV) is large enough for thermal stability of the ripple along the zigzag direction compared to one along the armchair direction at room temperature. (Supplementary Note 1).

Zigzag-directional ripples with nanometer-wavelength have also been observed in graphene on a different substrate, Cu(111)¹². Periodic corrugation in graphene has been known to modify the electron dispersion to be anisotropic around Dirac points. The influence of the crystallographic orientation of the ripple was not properly considered for the calculation though¹⁶. The ripple domains as patches of electronic superlattices do not only influence the mechanical properties of the graphene like friction but should also play an important role in the electrical transport characteristics. Therefore, we suggest that the influence of multi-domain ripples on the electrical transport of graphene on a substrate is worthwhile to be further investigated.

Conclusion

In summary, we have experimentally determined the ripple directions and crystallographic axes of single-layer graphene using cantilever torsion microscopy and angle-resolved photoemission spectroscopy, respectively. By comparing the results from the two techniques, we have demonstrated that the ripple is aligned along the zigzag direction of graphene. Theoretical calculations support the experimental results showing that a zigzag-directional ripple is energetically preferred to an armchair-directional one. Our results

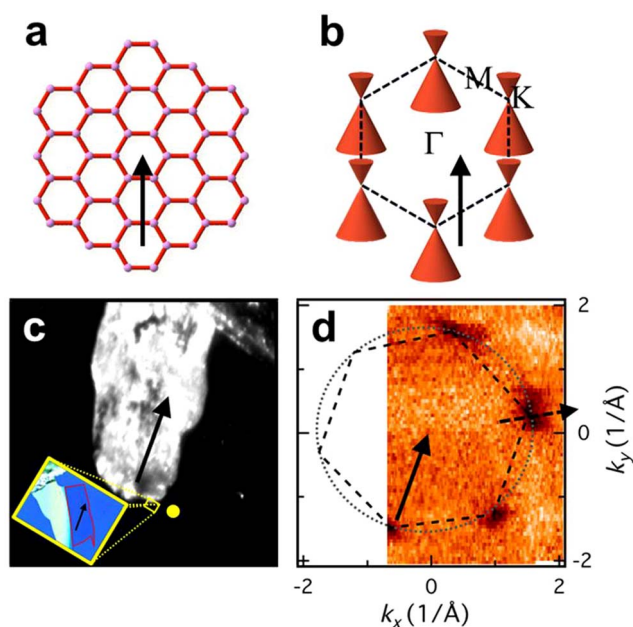


Figure 2 | Identification of crystallographic axis using ARPES measurements. (a) Lattice structure of graphene. (b) Hexagonal Brillouin zone with points of high symmetry indicated, showing the K and K' points coinciding with the Dirac points where the valence and the conduction bands meet. (c) Optical microscopy images and (d) ARPES image at the Fermi level. A large white area in (c) is silver paint and the MLG and SLG (magnified inset) is attached to it. The silver paint serves as an alignment mark. The solid arrows in (a–d) denote the zigzag direction of the graphene lattice in the real space.

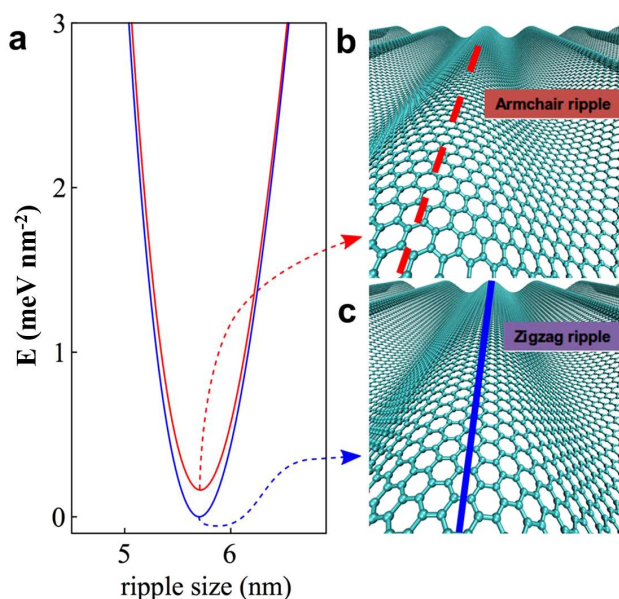


Figure 3 | Theoretical estimation of the formation energy for ripples. (a) The sum of the interaction energy between graphene and the substrate and the rippling energy of graphene due to the curvature as a function of the ripple width when the ripple is aligned along the zigzag (blue) or the armchair (red) direction. It shows that the zigzag-directional ripple has lower energy at the total energy minimum. Relaxed structures of graphene with (b) armchair- and (c) zigzag-directional ripples are obtained from *ab initio* calculations.

suggest that the non-destructive cantilever torsion microscopy is a practical tool for identifying the crystallographic axes of graphene at normal temperature and pressure, which is essential for fabrications of graphene-based devices with a good edge control.

Methods

Sample preparation. Graphene samples are prepared using the standard mechanical cleavage technique, using Kish graphite flakes on thermally oxidized silicon substrate (300 nm SiO_2) under ambient conditions. Graphene samples are sorted using optical microscopy. The number of graphene layers is confirmed using Raman spectroscopy. After each AFM experiment, the used graphene sample is stored in a high-vacuum chamber ($\sim 10^{-7}$ Torr) for several hours, and then, is kept in a sealed plastic pack with silica gel to keep the interface between graphene and the substrate dry. Silver paint is connected to the graphene to form an electrical contact, which prevents charge accumulation during ARPES measurements. The silver paint provides a reference position and direction for the sample during loading of the sample in carrying out CTM and ARPES measurements and comparing the ripple direction and crystallographic axis of SLG obtained through both methods.

AFM experiment. CTM images are obtained using the contact mode with a Seiko SPA-300HV AFM under ambient conditions. We use silicon AFM tips (Nanosensors PPP-LFMR with a spring constant of 0.2 N m^{-1}). Two kinds of CTM images are obtained by scanning the AFM tip perpendicular (T_{LON}) and parallel (T_{LAT}) to the cantilever body-length direction. Each ripple direction is determined by comparing cantilever torsions caused by aligned ripples which impede the AFM tip scanning during T_{LON} and T_{LAT} .

ARPES experiment. ARPES spectra are obtained at the Electronic Structure Factory end station (SES-R4000 analyzer) at Beamline 7 of the Advanced Light Source, Lawrence Berkeley National Laboratory. The sample is held under vacuum without any thermal treatment. During the measurements, the samples are kept at 300 K and the pressure is less than 2×10^{-10} Torr. A photon energy of 170 eV is used in the ARPES measurements giving overall resolutions of $\sim 100 \text{ meV}$ and $\sim 0.01 \text{ \AA}^{-1}$. Since the spot size of the synchrotron X-ray used in the ARPES measurement ($\sim 100 \mu\text{m}$) is slightly bigger than the dimensions of the whole SLG region ($30 \times 85 \mu\text{m}^2$), the measurement area covers both the SLG and MLG regions. The graphene flake preserves its rotational symmetry when its layer thickness increases. Each layer of bilayer graphene and MLG, as the stacking of two and more graphene monolayers, shifts its lattice laterally without rotation. Because the entire graphene sample was exfoliated from a single-

crystalline graphite crystal, both SLG and MLG regions have the same lateral crystallographic axis.

- Mermin, N. D. Crystalline order in two dimensions. *Phys. Rev.* **176**, 250–254 (1968).
- Mounet, N. & Marzari, N. First-principles determination of the structural, vibrational and thermodynamic properties of diamond, graphite, and derivatives. *Phys. Rev. B* **71**, 205214 (2005).
- Fasolino, A. J., Los, H. & Katsnelson, M. I. Intrinsic ripples in graphene. *Nat. Mater.* **6**, 858–861 (2007).
- Guinea, F., Katsnelson, M. I. & Vozmediano, M. A. H. Midgap states and charge inhomogeneities in corrugated graphene. *Phys. Rev. B* **77**, 075422 (2008).
- He, Y. Z. *et al.* Dynamic ripples in single layer graphene. *Appl. Phys. Lett.* **98**, 063101 (2011).
- Wang, Z. & Devel, M. Periodic ripples in suspended graphene. *Phys. Rev. B* **83**, 125422 (2011).
- Morozov, S. V. *et al.* Strong suppression of Weak Localization in graphene. *Phys. Rev. Lett.* **97**, 016801 (2006).
- Chen, C.-C. *et al.* Raman spectroscopy of ripple formation in suspended graphene. *Nano Lett.* **9**, 4172–4176 (2009).
- Geringer, V. *et al.* Morgenstern, Intrinsic and extrinsic corrugation of monolayer graphene deposited on SiO_2 . *Phys. Rev. Lett.* **102**, 076102 (2009).
- Bao, W. *et al.* Controlled ripple texturing of suspended graphene and ultrathin graphite membranes. *Nat. Nanotechnol.* **4**, 562–566 (2009).
- Locatelli, A. *et al.* Corrugation in exfoliated graphene: An electron microscopy and diffraction study. *ACS Nano* **4**, 4879–4889 (2010).
- Tapasztó, L. *et al.* Breakdown of continuum mechanics for nanometre-wavelength rippling of graphene. *Nat. Phys.* **8**, 739 (2012).
- de Juan, F., Cortijo, A., Vozmediano, M. A. H. & Cano, A. Aharonov-Bohm interferences from local deformations in graphene. *Nature Phys.* **7**, 810–815 (2011).
- Levy, N. *et al.* Strain-induced pseudo-magnetic fields greater than 300 Tesla in graphene nanobubbles. *Science* **329**, 544–547 (2010).
- Isacsson, A. *et al.* Electronic superlattices in corrugated graphene. *Phys. Rev. B* **77**, 035423 (2008).
- Park, C. H. *et al.* Anisotropic behavior of massless Dirac fermions in graphene under periodic potentials. *Nature Phys.* **4**, 213–217 (2008).
- Choi, J. S. *et al.* Friction anisotropy-driven domain imaging on exfoliated monolayer graphene. *Science* **333**, 607–610 (2011).
- Choi, J. S. *et al.* Facile characterization of ripple domains on exfoliated graphene. *Rev. Sci. Instrum.* **83**, 073905 (2012).
- Morozov, S. V. *et al.* Strong suppression of weak localization in graphene. *Phys. Rev. Lett.* **97**, 016801 (2006).
- Son, Y.-W., Cohen, M. L. & Louie, S. G. Half-metallic graphene nanoribbons. *Nature* **444**, 347–349 (2006).
- Son, Y.-W., Cohen, M. L. & Louie, S. G. Energy gaps in graphene nanoribbons. *Phys. Rev. Lett.* **97**, 216803 (2006).
- Ritter, K. A. & Lyding, J. W. The influence of edge structure on the electronic properties of graphene quantum dots and nanoribbons. *Nat. Mater.* **8**, 235–242 (2009).
- Enoki, T., Fujii, S. & Takai, K. Zigzag and armchair edges in graphene. *Carbon* **50**, 3141–3145 (2012).
- Campione, M. & Fumagalli, E. Friction anisotropy of the surface of organic crystals and its impact on scanning force microscopy. *Phys. Rev. Lett.* **105**, 166103 (2010).
- Kalihar, V. *et al.* Grain orientation mapping of polycrystalline organic semiconductor films by transverse shear microscopy. *Adv. Mater.* **20**, 4033–4039 (2008).
- Flesch, H.-G. *et al.* Microstructure and phase behavior of a quinquethiophene-based self-assembled monolayer as a function of temperature. *J. Phys. Chem. C* **115**, 22925–22930 (2011).
- Marsden, A. J., Phillips, M. & Wilson, N. R. Friction force microscopy: a simple technique for identifying graphene on rough substrates and mapping the orientation of graphene grains on copper. *Nanotechnol.* **24**, 255704 (2013).
- Filleter, T. & Bennewitz, R. Structural and frictional properties of graphene films on SiC(0001) studied by atomic force microscopy. *Phys. Rev. B* **81**, 155412 (2010).
- Lee, C. *et al.* Frictional characteristics of atomically thin sheets. *Science* **328**, 76–80 (2010).
- Bostwick, A. *et al.* Experimental studies of the electronic structure of graphene. *Prog. Surf. Sci.* **84**, 380–413 (2009).
- Knox, K. R. *et al.* Making angle-resolved photoemission measurements on corrugated monolayer crystals: Suspended exfoliated single-crystal graphene. *Phys. Rev. B* **84**, 115401 (2011).
- Sprinkle, M. *et al.* First direct observation of a nearly ideal graphene band structure. *Phys. Rev. Lett.* **103**, 226803 (2009).
- Varchon, F. *et al.* Electronic structure of epitaxial graphene layers on SiC: Effect of the substrate. *Phys. Rev. Lett.* **99**, 126805 (2007).
- Zhou, S. Y. *et al.* Substrate-induced bandgap opening in epitaxial graphene. *Nature Mater.* **6**, 770 (2007).
- Ohta, T. *et al.* Controlling the electronic structure of bilayer graphene. *Science* **313**, 951 (2006).



36. Yoon, D., Son, Y.-W. & Cheong, H. Negative thermal expansion coefficient of graphene measured by Raman spectroscopy. *Nano Lett.* **11**, 3227–3231 (2011).
37. Lee, C. *et al.* Measurement of the elastic properties and intrinsic strength of monolayer graphene. *Science* **321**, 385 (2008).
38. Abedpour, N., Asgari, R. & Reza Rahimi Tabar, M. Irreversibility in response acting on graphene sheets. *Phys. Rev. Lett.* **104**, 196804 (2010).
39. Chang, T., Geng, J. & Guo, X. Chirality- and size-dependent elastic properties of single-walled carbon nanotubes. *App. Phys. Lett.* **87**, 251929 (2005).
40. Koenig, S. P. *et al.* Ultrastrong adhesion of graphene membranes. *Nat. Nanotech.* **6**, 543–546 (2011).

Acknowledgments

This work is supported by the National Research Foundation of Korea(NRF) grants funded by the Korea government(MSIP) (Grant No. 2013R1A3A2042120, 2011-0030229, 2011-0031660, 2014R1A1A1002868, and 2008-0061893(QMMRC)). The Advanced Light Source is supported by the Director, Office of Science, Office of Basic Energy Sciences, of the US Department of Energy under contract no. DE-AC02-05CH11231. C.-G. C. acknowledges the Creative Research Program of the ETRI (14ZE1110) of Korea. Computation is supported by the CAC of KIAS.

Author contributions

Y.J.C. and B.H.P. planned the projects; J.S.C., Y.J.C., B.H.P., A.B. and E.R. designed the experiments; J.S.C., Y.P., M.J.L., I.-S.B. and J.-S.K. carried out sample preparation and AFM measurements; Y.J.C., A.B. and E.R. carried out the ARPES experiments; S.W. and Y.-W.S. performed and analyzed the calculations; J.S.C., Y.J.C., S.W., B.H.P., Y.-W.S., C.-G.C., A.B. and E.R. interpreted the results; All authors discussed the results and commented on the manuscript.

Additional information

Supplementary information accompanies this paper at <http://www.nature.com/scientificreports>

Competing financial interests: The authors declare no competing financial interests.

How to cite this article: Choi, J.S. *et al.* Correlation between micrometer-scale ripple alignment and atomic-scale crystallographic orientation of monolayer graphene. *Sci. Rep.* **4**, 7263; DOI:10.1038/srep07263 (2014).



This work is licensed under a Creative Commons Attribution-NonCommercial-NoDerivs 4.0 International License. The images or other third party material in this article are included in the article's Creative Commons license, unless indicated otherwise in the credit line; if the material is not included under the Creative Commons license, users will need to obtain permission from the license holder in order to reproduce the material. To view a copy of this license, visit <http://creativecommons.org/licenses/by-nc-nd/4.0/>